7th Annual International IEEE EMBS Conference on Neural Engineering
Montpellier, France, 22 - 24 April, 2015

Modeling electrode place discrimination in cochlear implants: Analysis of the influence of electrode array insertion depth

Xiao Gao[1], David B. Grayden[2] and Mark D. McDonnell[3]

Abstract— **Cochlear implants provide functional hearing to people who are profoundly deaf or hearing impaired by replacing the function of missing inner hair cells with an array of stimulating electrodes. Previous studies developed a modeling framework for predicting the optimal number of electrodes, as well as the optimal locations and usage probabilities of electrodes, from an information theoretic perspective. However, the information theoretic method does not quantify the performance of electrode place discrimination. In this paper, we apply a so-called 'extreme-learning machine' to the cochlear implant model to calculate the electrode classification error rates. We also investigate the locations along the electrode array where errors are most likely to occur. We conclude based on our model that i) the classification error rate increases with increasing number of electrodes and the classification errors occur predominantly between adjacent electrodes, ii) by inserting the electrode array deeper into the cochlea, more electrode locations can be distinguished and the electrodes for which most errors occur are determined by the distance and spiral twirling angle between adjacent electrodes.**

I. INTRODUCTION

A cochlear implant [1] is an electronic biomedical device designed to bypass damaged inner hair cells by direct electrical stimulation of auditory nerve fibers. Modern cochlear implants consist of up to 22 electrodes to replace the function of over 3000 inner hair cells. Although many cochlear implant recipients perceive speech well in quiet conditions, their ability to understand speech in noisy environments and to appreciate music is still limited. Increasing the number of electrodes does not improve hearing performance, and this is thought to be mainly due to *current spread*, which causes electrodes that are close together to stimulate overlapping populations of auditory nerve fibers [2]. However, recent research [3] suggests that more than 100 individual spectral channels may be perceived by cochlear implant users via *current steering*. In this paper, we aim to investigate how many electrode locations can be distinguished using a channel model of cochlear implants.

M. D. McDonnell was supported by an Australian Research Fellowship funded by the Australian Research Council (project number DP1093425).

[1]X. Gao is with the Computational and Theoretical Neuroscience Laboratory, Institute for Telecommunications Research, University of South Australia, Mawson Lakes SA 5095, Australia. xiao.gao@mymail.unisa.edu.au

[2]D. B. Grayden is with the NeuroEngineering Laboratory, Department of Electrical and Electronic Engineering, and the Centre for Neural Engineering, University of Melbourne, VIC 3010, Australia. grayden@unimelb.edu.au

[3]M. D. McDonnell is with the Computational and Theoretical Neuroscience Laboratory, Institute for Telecommunications Research, University of South Australia, Mawson Lakes SA 5095, Australia. mark.mcdonnell@unisa.edu.au

Electrode place discrimination is equivalent to a multi-class classification problem. We address this problem by adapting previous studies that established a modeling framework for predicting the optimal number of electrodes, as well as finding the optimal locations and usage probabilities of electrodes from an information theoretic perspective [4]–[7]. In these works, the interface between the electrode array and the auditory nerve is conceptualized as a communication channel for a discrete memoryless source, which enables the calculation of the mutual information between a channel input random variable (choice of electrodes) and a channel output random variable (a function of the active nerve fibers in response to an electrode choice). Based on the assumption that an increased mutual information leads to increased electrode place discrimination [8], the information theoretic models predicts the "optimal" number of electrodes as that which achieves the maximum mutual information [4], [5].

However, the mutual information only represents the statistical correlations between the outcomes of channel inputs and outputs in the model, whereas to quantify the performance of place discrimination, the channel output random variables need to be processed to an actual decision. That is, the decision on which electrode is stimulated in response to an activation pattern in the fibers.

The goals of this paper, therefore, are to investigate three important and clinically relevant problems: i) whether more electrode locations can be distinguished by inserting cochlear implant electrode arrays deeper into the cochlea, ii) the locations along the electrode array where most errors occur, and iii) classification error rates for each electrode location. To achieve these goals, we first update two individual components of the modeling framework [4] (see Sec. I-B); namely we use a realistic spiral geometry model, and we choose maximum current levels tailored individually for each electrode. Then instead of calculating mutual information, we apply a discriminative classifier (a recently developed variant of an artificial neural network, known as an extreme learning machine (ELM) [9]) to simulations of the population activity of the auditory nerve in the model, in order to predict the location of the stimulating electrode. The premise is that if an engineered classifier cannot determine the cause of a particular pattern, then neither will the real biological system.

Before proceeding, the following subsections describe the structure of the modeling framework in [4] and the updates that we made to the modeling framework in this paper.

A. Overview of the channel model of cochlear implants

The model of [4] has five components:

1) geometry model of fiber and electrode locations;
2) stochastic action potential generation model in individual auditory nerve fibers;
3) electrode current spread model;
4) dependence of loudness perception model on overall auditory nerve activity;
5) information theoretic model of place discrimination.

It is straightforward to introduce improvements or replacements to any of the individual components in this modeling framework while maintaining the core concepts of the modeling framework [4], [5].

B. Updates to the modeling framework

In this paper, we maintain components 2 and 3 (from [2]). The following changes are made for components 1, 4 and 5:

- For component 1, we replace the linear electrode-to-fiber geometry model with a helical geometry model [10] since the actual human cochlea and the implanted electrode array form a three-dimensional spiral.
- For component 4, instead of choosing the same current level for each electrode [4], we choose different maximum current levels for each electrode such that stimulation of each electrode causes approximately 10% of the auditory nerve fibers to generate action potentials.
- For component 5, we keep the general concept of the electrode location discrimination model in [4]. The channel input is defined as the locations of electrodes X_e ($X_e = x_{e,j}, j = 1, 2, \ldots, M$), where M is the number of electrodes in the array. The channel output is defined as a vector of outcomes for a total of N auditory nerve fibers (the fiber spiking pattern), which is denoted as $(Y_i)_{i=1,2,\ldots,N}$. A Bernoulli random variable $Y_i \in \{0, 1\}$ denotes whether or not fiber i produces an action potential in response to electrode current $C_{f,i}$.

For more detail of each individual component of the modeling framework, see [4], [5], and [10].

In this paper, an activation pattern $\mathbf{Y}$ is processed to make a decision on which electrode is stimulated that caused this pattern. To make this decision, each example pattern, $\mathbf{Y}$, is assigned to one of the M electrodes, which can be referred to as a multi-class classification problem [11]. The performance of place discrimination is then estimated by calculating the correct classification rates by simulating many repeated stimulations of each electrode using the model.

II. AN ELM CLASSIFIER FOR ELECTRODE PLACE DISCRIMINATION

We adapt the ELM method of [9] to solve the electrode place discrimination problem. Specifically, we use a multi-class classifier with multi-outputs in this paper; i.e., M–class classifier with M output nodes.

Two phases are involved in the classification of fiber activation samples: 1) training an ELM classifier and 2) testing the classification performance using the trained ELM classifier. Before we present the training phase and testing phase, we introduce some parameters that define the dimensions of the classifier.

- The dimension of each training vector (equal to the number of fibers) is defined as N.
- The number of hidden layer neurons is defined as L.
- The number of distinct labels of training vectors (equal to the number of electrodes) is defined as M.

We also define two matrices in order to map the fiber activation samples (the input vectors) into the indices of electrodes (the prediction vectors).

- The input weight matrix $\mathbf{W}_{\text{in}}$ (of size $L \times N$) maps the data from the N-dimensional input space to the L-dimensional hidden-layer feature space.
- The output weight matrix $\mathbf{W}_{\text{out}}$ (of size $M \times L$) maps the L-dimensional hidden-layer activations to M-dimensional predication vectors.

In our ELM classifier, the input weights are randomly chosen from uniform distribution on the interval $[-1, 1]$.

A. Training an ELM classifier

Let the training vectors be $\mathbf{T} = [\mathbf{t}_1, \ldots, \mathbf{t}_i, \ldots, \mathbf{t}_{P_1}]$, where P_1 is the number of training vectors and $\mathbf{t}_i$ (of size $N \times 1$) is a single training vector which represents an activation pattern $\mathbf{Y}$ as described in Sec. I-B. We denote $\mathbf{V}$ as the labels of each training sample. For simplicity of calculation, we define $\mathbf{V} = [\mathbf{v}_1, \ldots, \mathbf{v}_i, \ldots, \mathbf{v}_{P_1}]$, where $\mathbf{v}_i$ has size $M \times 1$. In $\mathbf{v}_i$, only one element is a 1 corresponding to the label of training vector $\mathbf{t}_i$ and all other elements are 0. The label of $\mathbf{t}_i$ represents which particular electrode is stimulated to produce the training points in $\mathbf{t}_i$.

We define $\mathbf{Z}$ as the prediction vectors

$$\mathbf{Z} = \mathbf{W}_{\text{out}} f(\mathbf{W}_{\text{in}} \mathbf{T}), \tag{1}$$

where $\mathbf{W}_{\text{in}}\mathbf{T}$ is the hidden layer neuron activations, and $f(\cdot)$ is the termwise ($L \times P_1 \to L \times P_1$) neuron activation function. In this paper, the absolute value function is used for the neuron activations. Note that, other nonlinear activation functions may also be used.

By training the classifier, we seek to find $\mathbf{W}_{\text{out}}$ that minimizes the mean square error between $\mathbf{V}$ and $\mathbf{Z}$.

B. Classification using the trained ELM classifier

We define testing vectors as $\mathbf{T}' = [\mathbf{t}'_1, \ldots, \mathbf{t}'_i, \ldots, \mathbf{t}'_{P_2}]$, where P_2 is the number of testing vectors and $\mathbf{t}'_i$ (of size $N \times 1$) represents a single test vector.

Then the prediction vectors for the testing phase is defined as

$$\mathbf{Z}' = \mathbf{W}_{\text{out}} f(\mathbf{W}_{\text{in}} \mathbf{T}'), \tag{2}$$

where $\mathbf{W}_{\text{out}}$ is obtained in the training phase. The classification decision for testing vector i is made from $\mathbf{Z}'$ by choosing the maximum element in its i–th column. This corresponds to making a decision of which electrode generated the fiber spiking pattern that generated $\mathbf{t}'_i$.

III. RESULTS

We now quantify the classification performance by investigating the correct classification rates for different spiral angles of electrode array in Sec. III-A and where the errors happen along the array in Sec. III-B.

Before presenting the results, we choose a set of parameters for the cochlear implant model as an example case. The distance between the electrode array and the auditory nerve fibers is $r = 2$ mm. We use $N = 3000$ as the number of surviving auditory nerve fibers, and fibers have identical parameters as in [4] and are nonuniformly located along the cochlea according to a model of the actual location distribution. The electrodes are uniformly spaced along the unwrapped length of the array, and the electrode stimulation strategy is bipolar stimulation.

A. Percentage of correct classification

The total spiral angle of a human cochlea is approximately 5π radians. We choose two example spiral angles of the electrode array, $\alpha = \{2\pi, 3\pi\}$, since the electrode array are not usually implanted very deep into the cochlea. The number of hidden-layer neurons is chosen as $L = 1500$, since this achieves the approximately optimal classification performance in our model. We generate 400 sets of fiber activation patterns per electrode. Of these, 90% are used as training data, the rest are used for testing.

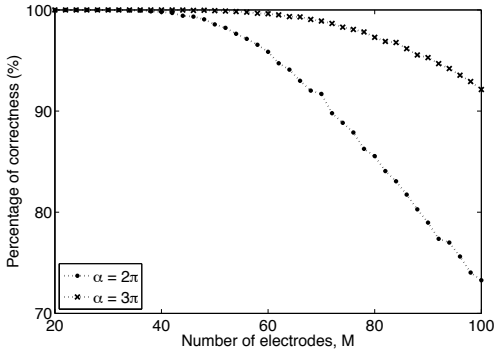

Fig. 1. Comparison of the percentage of correct classification versus the number of electrodes, M, for two cases of the spiral angles of electrode array, $\alpha = \{2\pi, 3\pi\}$.

Fig. 1 compares the percentage of correct classification versus the number of electrodes for two cases of the spiral angles of electrode array, $\alpha = \{2\pi, 3\pi\}$. The correct classification rates decrease with increasing numbers of electrode for both insertion depths. Specifically, the gap of correct classification rates between the $\alpha = 2\pi$ case and the $\alpha = 3\pi$ case increases with increasing number of electrodes.

We notice that the unwrapped length of the electrode array for the $\alpha = 2\pi$ model is about 9.5 mm shorter than for the $\alpha = 3\pi$ model (for calculation details, see [10]). In other words, the distance between adjacent electrodes d for $\alpha = 2\pi$ is approximately $9.5/M$ mm shorter than for $\alpha = 3\pi$. We now investigate how the distance between adjacent electrodes impacts on the classification performance.

Fig. 2 compares the percentage of correct classification versus the distance between adjacent electrodes. We observe

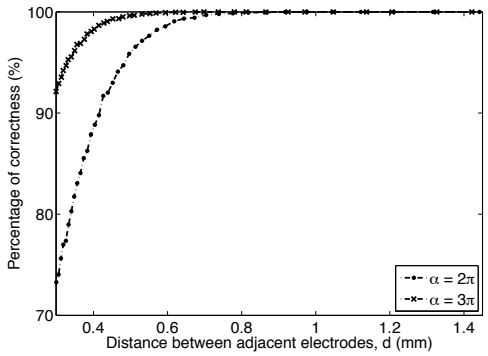

Fig. 2. Comparison of the percentage of correct classification versus the distance between each adjacent electrode, d, for two cases of the spiral angles of electrode array, $\alpha = \{2\pi, 3\pi\}$.

that, compared to the $\alpha = 3\pi$ model, the correct classification rate for the $\alpha = 3\pi$ model decreases more slowly with decreasing d. We note that, for a fixed d, the $\alpha = 3\pi$ array always has more electrodes than the $\alpha = 2\pi$ array. We discuss these results in Sec. IV after visualizing the classification error rates for each electrode in Sec. III-B.

B. Classification errors for each electrode location

Fig. 3 shows the classification error rates of each electrode along the array. Row **A** shows the case of $\alpha = 2\pi$, row **B** shows the case of $\alpha = 3\pi$. In each row, the columns from the left to right represent the number of electrodes, $M = \{40, 70, 100\}$, respectively. The horizontal axis of each matrix indicates the index of the actual stimulated electrode, m, the vertical axis indicates the index of the electrode that is chosen by the ELM classifier, m'. The matrix element at position (m, m') gives the estimated probability that electrode m is predicted as electrode m'. To clearly present the error probabilities, the probabilities that elements at position $m = m'$ (correct classification) are not shown in this figure. In this paper, we number the electrodes from the basal end to the apical end in sequence.

For both $\alpha = 2\pi$ and $\alpha = 3\pi$, the errors increase with increasing numbers of electrodes. Incorrect classifications happens most frequently between adjacent electrodes. For the $\alpha = 3\pi$ model, the errors are closer to the basal end of the array than $\alpha = 2\pi$, and the error probabilities of the basal electrodes are higher than the apical electrodes.

IV. DISCUSSION

A. Does a longer electrode array lead to better electrode place discrimination?

The $\alpha = 3\pi$ model always achieves better classification performance than the $\alpha = 2\pi$ model except where the correct classification rate is approximately 100%. As mentioned in Sec. III-A, the $\alpha = 3\pi$ electrode array is longer than the $\alpha = 2\pi$ array. Thus, with the same number of electrodes, current spread affects more adjacent electrodes for the $\alpha = 2\pi$ case since the distance between them is smaller.

We then investigated how the classification performance changed versus d. Fig. 2 indicates that the longer electrode array ($\alpha = 3\pi$) helps with distinguishing more electrode

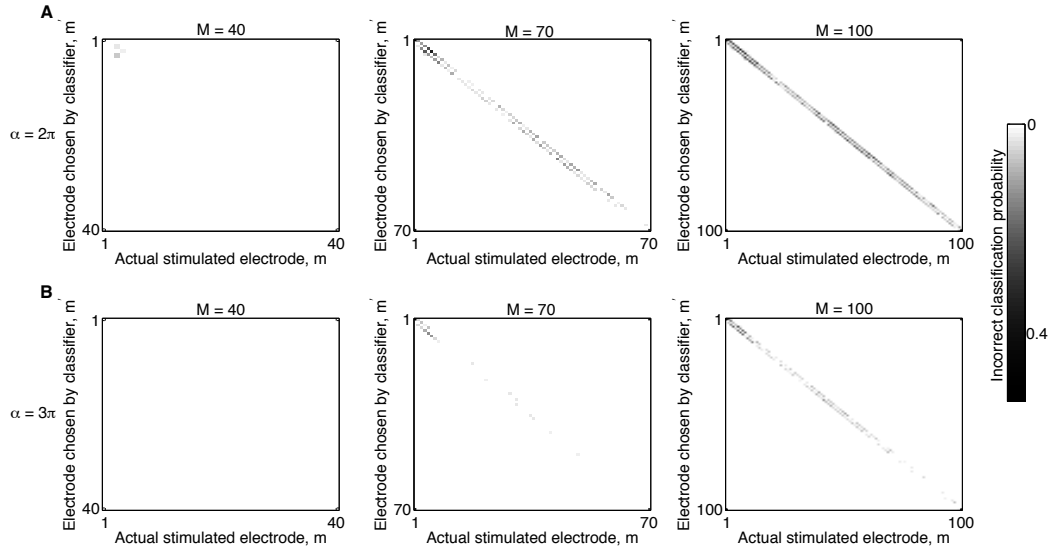

Fig. 3. Confusion matrices that show the classification error rates of each electrode along the array. Row **A** shows the case $\alpha = 2\pi$, row **B** shows the case $\alpha = 3\pi$. In each row, the columns from the left to right represent the number of electrodes, $M = \{40, 70, 100\}$, respectively. The horizontal axis of each matrix indicates the index of the actual stimulated electrode, m, the vertical axis indicates the index of the electrode that is chosen by the ELM classifier, m'. The matrix element at position (m, m') gives the probability that electrode m is predicted as electrode m'.

locations. We observe in Fig. 3 that by inserting electrodes into the second turn of the cochlea, the electrodes located at the second turn stimulate less overlapping populations of fibers compared with electrodes on the first turn. We conclude this is the reason that the $\alpha = 3\pi$ array has better place discrimination in the model.

B. Where do the classification errors occur?

One phenomenon observed in Fig. 3 is that for both cases of electrode spiral angles, all errors happen between adjacent electrodes. Since current spread causes adjacent electrodes to stimulate the most overlapping populations of fibers, it is not surprising that most errors are those where the chosen electrode is the one adjacent to the actual one.

Another phenomenon is that for the $\alpha = 3\pi$ array, the errors are predominantly at the basal end of the array. We recall that the electrodes are assumed uniformly located along the unwrapped length of the array. In this case, the twirling angle between adjacent electrodes, denoted as θ, gradually increases from the basal electrodes to the apical electrodes. This is because the radius decreases from the first turn to the second turn of the array. We have verified that if the electrode locations are determined instead by equally spaced twirling angles, the most errors instead occur closer to the apical end of the array (results not shown).

In summary, in this paper, we investigated how the classification performance changes with the number of electrodes and the distance between electrodes for different electrode array insertion depth. We inferred that inserting the electrode array deeper into the cochlea could help with better electrode place discrimination performance. We also found that where the errors happen along the electrode array is affected not only by the distance between electrodes but also the twirling angle between electrodes. Some valuable future work could be done to provide more precise estimation of the classification performance by i) applying a biologically plausible single neuron model in the classifier, ii) improving or changing individual components in the cochlear implants model, and iii) undertaking experimental studies to validate the model's predictions.

REFERENCES

[1] B. S. Wilson, M. F. Dorman, "Cochlear implants: A remarkable past and a brilliant future," *Hearing Research*, vol. 242, pp. 3–21, 2008.

[2] I. C. Bruce, M. W. White, L. S. Irlicht, S. J. O'Leary, and G. M. Clark, "The effects of stochastic neural activity in a model predicting intensity perception with cochlear implants: Low-Rate stimulation," *IEEE Transactions on Biomedical Engineering*, vol. 46, pp. 1393–1403, 1999.

[3] D. B. Koch, M. Downing, M. J. Osberger, and L. Litvak, "Using current steering to increase spectral resolution in CII and HiRes 90K users," *Ear and Hearing*, vol. 28, pp. 38S–41S, 2007.

[4] M. D. McDonnell, A. N. Burkitt, D. B. Grayden, H. Meffin, and A. J. Grant, "A channel model for inferring the optimal number of electrodes for future cochlear implants," *IEEE Transactions on Information Theory*, vol. 56, pp. 928–940, 2010.

[5] X. Gao, D. B. Grayden, and M. D. McDonnell, "Stochastic information transfer from cochlear implant electrodes to auditory nerve fibers," *Physical Review E*, vol. 90, p. 022722, 2014.

[6] X. Gao, D. B. Grayden, and M. D. McDonnell, "Information theoretic optimization of cochlear implant electrode usage probabilities," in *35th Annual International Conference of the IEEE Engineering in Medicine and Biology Society*, 2013, pp. 5974–5977.

[7] X. Gao, D. B. Grayden, and M. D. McDonnell, "Inferring the dynamic range of electrode current by using an information theoretic model of cochlear implant stimulation," in *IEEE Information Theory Workshop*, 2014, pp. 347–351.

[8] A. Borst and F. E. Theunissen, "Information theory and neural coding," *Nature Neuroscience*, vol. 2, pp. 947–957, 1999.

[9] G. B. Huang, H. Zhou, X. Ding, and R. Zhang, "Extreme learning machine for regression and multiclass classification," *IEEE Transactions on Systems, Man, and Cybernetics, Part B: Cybernetics*, vol. 42, pp. 513–529, 2012.

[10] A. S. Moroz, M. D. McDonnell, A. N. Burkitt, D. B. Grayden, and H. Meffin, "Information theoretic inference of the optimal number of electrodes for future cochlear implants using a spiral cochlea model," in *34th Annual International Conference of the IEEE Engineering in Medicine and Biology Society*, 2012, pp. 2965–2968.

[11] C. M. Bishop, *Pattern recognition and machine learning*. Springer, 2007.